Evaluation of the bearing capacity of suction bucket foundations used for offshore wind turbines using finite element modeling

Évaluation de la capacité portante de caissons d'aspiration fondation utilisé pour éolienne offshore à l'aide modélisation par éléments finis

Pouyan Bagheri
Civil and Environmental Engineering, Pusan National University, Korea, pouyan.bagheri@gmail.com
Su Won Son
Civil and Environmental Engineering, Pusan National University, Korea
Jin Man Kim
Civil and Environmental Engineering, Pusan National University, Korea

ABSTRACT: Recently offshore wind power has been widely used as a valuable and renewable source of energy. The suction buckets are considered as economically efficient and easy installed foundations for offshore wind turbines. Since the large horizontal force and overturning moment apply to this type of foundation, this study focuses on the bearing behavior of bucket foundation installed on dense and medium dense sand with regard to different eccentricities by using finite element method. Three embedment ratio of bucket foundation were considered to analyze the ultimate horizontal load and moment. A parametric analysis of suction caisson reveals that the ultimate capacity substantially depends on bucket dimensions and load conditions. Dimensionless bearing capacity curves are presented for preliminary design in such type of soils.

RÉSUMÉ : Récemment, l'énergie éolienne offshore a largement servi comme source d'énergie précieuse et renouvelable. Les caissons d'aspiration sont vus comme rentables et font aisément office de fondation aux éoliennes offshore. Comme une grande force horizontale et un moment de torsion s'appliquent sur ce type de fondation, cette étude s'intéressera à la portance de ces caissons installé dans des sables denses et moyen-denses et leurs différentes excentricités en fonction, le tout en se servant de la simulation numérique et la méthode des éléments finis. Afin d'analyser la charge horizontale et le moment de torsion maximum, trois rapports d'enfouissement ont été choisis. Une analyse paramétrique des caissons d'aspiration révèlera que leur capacité maximale dépend considérablement de leurs dimensions et des conditions de charge. Des courbes adimensionnelles seront présentées en vue de la conception préliminaire en fonction de tel type de sol.

KEYWORDS: Offshore wind turbine, suction bucket foundation, load-bearing capacity, sand.

1 INTRODUCTION

The use of offshore wind energy is generally suggested to play a significant role in the future electricity supply. To make offshore wind energy competitive in the market, the cost-effectiveness and installation technology should be properly taken into account. Optimum foundation solutions is a big challenge for geotechnical engineers. Suction bucket foundation can be a cost-reducing and easy installed foundation for offshore wind turbines (Achmus et al. 2013). Traditionally bucket caissons have been used for decades in oil and gas industry as a foundation for jackets (Bye et al. 1995). Due to different loading conditions in offshore wind turbines, strong attentions are needed to be paid in the design of such structures.
Most previous studies have been focused on both monotonic and cyclic response of the bucket foundation using laboratory experimental tests (Bryne and Houlsby 2004, Villalobos et al. 2009) and field tests (Houlsby et al. 2005, Houlsby and Bryne 2000). By conducting small-scale laboratory test, (Bryne and Houlsby 2004) investigated bucket foundation response under combination of various loadings for both monotonic and cyclic conditions. They found that there is highly correlation between bucket response and vertical loading conditions. (Houlsby et al. 2005) performed large-scale field tests on the model of bucket foundation to predict the cyclic response of bucket foundation under horizontal and vertical loads. (Houlsby and Byrne 2000) carried out large-scale field tests to check the applicability of bucket foundations for offshore wind turbines. They reported the loading conditions from wind turbines are quite differenet from the offshore structures in oil industries.
Few numerical analysis studies have been performed to predict the loading response and bearing behavior of the suction caissons. (Zhang et al. 2010) by using an upper bound limit method, estimated the load capacity for bucket foundations. By utilizing finite element method, (Achmus et al. 2013) evaluated the horizontal and moment load capacity of bucket foundation in sandy soil.
In spite of investigations reported in the literature on the bearing behavior of bucket foundations used for offshore wind turbines, it is not yet totally clarified the bucket behavior and soil supporting the bucket under various loading conditions and bucket geometries. Hence, in this study, FE analysis was conducted to assess the bearing capacity of the bucket foundation and the response of soil supporting the bucket subjected to the monotonic loading.

2 FINITE ELEMENT MODEL

In this study, a three-dimensional finite element (FE) model was developed and used to analyze the bearing behavior of suction caisson and the soil supporting the bucket. The finite element program Plaxis 3D (Brinkgreve 2012) was utilized in the simulation.
A bucket foundation is a steel cylinder with diameter D, skirt length L and skirt thickness t_s, capped by a heavily stiffened upper steel lid. To reduce the computational effort and with regard to the symmetrical nature of the problem, only one-half of the bucket foundation was modeled. For simulation of soil, the Hardening Soil constitutive model was used. The formulation of the Hardening Soil model is in fact originated from the hyperbolic relationship between the vertical strain and

the deviatoric stress. Sand soil with two different densities were considered for modeling. Soil properties were determined using previous study already by (Ryu 2014) as well as the given equations in Plaxis 3D program manual (Brinkgreve 2012) (Table 1). Interface elements were utilized at caisson-soil interfaces. For modeling of the constitutive behavior of the soil and interface, the elastic-perfectly plastic stress-strain relationship and Mohr-Coulomb failure criterion was employed. Mesh convergence and physical boundary domain analusis were carried out to ensure the sufficient accuracy of the results and avoid the boundary conditions effect. Figure 1 shows the three-dimensional view of the numerical model with geometrical properties.

Note that to simplify the investigations, only one soil type with different densities was considered for modeling. Moreover, lack of consideration of layered soils with the shape of each layer is another eliminated factor in this study. Additionally, the effect of installation procedure in addition to the long-term cyclic and fatigue loading were also eliminated. Therefore, it is recommended to consider the mentioned factors in the future studies.

The bucket was simulated using steel plate element. The skirt thickness of the foundation was taken as *30 mm*, which is a typical thickness of the buckets in practice. The modulus of elasticity (*E), 210 GPa* and Poisson's ratio (*υ*), *0.3* were employed for the steel properties. The steel unit weight (*γ*) was also set to *77 kN/m*^{3}. A very large modulus of elasticity (*E=210×10* ^{6} *GPa*) with bucket lid thickness of *100 mm* were employed to the bucket lid in order to consider the rigid behavior of the bucket due to the stiffeners placed on the upper side of the bucket.

Table 1. Soil properties.

Soil type (sand)	*Medium dense*	*Dense*
Unit weight γ (*kN/m*^{3})	18.5	20
Secant stiffness (*kN/m*^{2})	74,536	110,110
Tangent stiffness (*kN/m*^{2})	59,629	88,088
Unloading/Reloading Stiffness (*kN/m*^{2})	223,608	330,330
Effective cohesion *C'* (*kN/m*^{2})	0.1	0.1
Effective angle of friction φ (°)	35	39
Angle of dilatancy ψ (°)	5	9
Relative density (%)	60	85

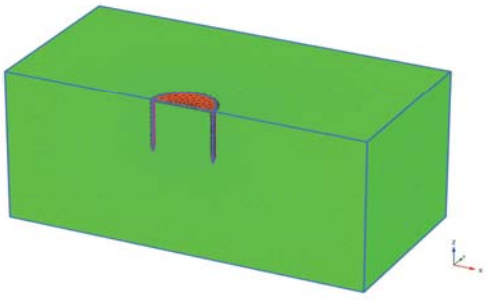

Figure 1. Finite element model of a suction bucket foundation.

The numerical analyses were conducted in several calculation phases. In initial phase, geostatic stresses comprising the only soil elements were calculated by applying the gravity loading. The predefined elements applied for the bucket and tower structures were subsequently replaced by steel plate material in the installation phase. In the next calculation phase, a vertical dead load *V* of *10000 kN* which is typical load for a large *5* MW offshore wind turbine, considering the super-structure of wind energy converter system was applied on the center of the bucket lid. The following phases comprise application of the horizontal load and overturning moment simultaneously with respect to different load eccentricities. The horizontal load and overturning moment were increased gradually to define the ultimate load and overturning moment capacity of the bucket foundation.

3 SIMULATION RESULTS

3.1 *Bucket rotation and displacement*

A bucket with diameter *D* of *14 m* and skirt length *L* of *7*, *10.5* and *14 m* which represent the embedment ratio *L/D* of *0.5*, *0.75*, *1* were considered for simulation modeling. Push-over analysis was used for a wide range of load eccentricities (*h=0 m, 5 m, 10 m, 20 m, 40 m, 70 m, 100 m*). Horizontal load-displacement (*H-y*) and overturning moment-rotation (*M-θ*) relations for an exemplary bucket dimension with embedment ratio (*L/D=0.75*) for dense sandy soil are displayed in Figures 2 and 3. As to be expected, the load eccentricity has a considerable effect on both the ultimate horizontal load and overturning moment capacities. The highest ultimate horizontal loading capacity was occurred with no load eccentricity *h=0 m*.

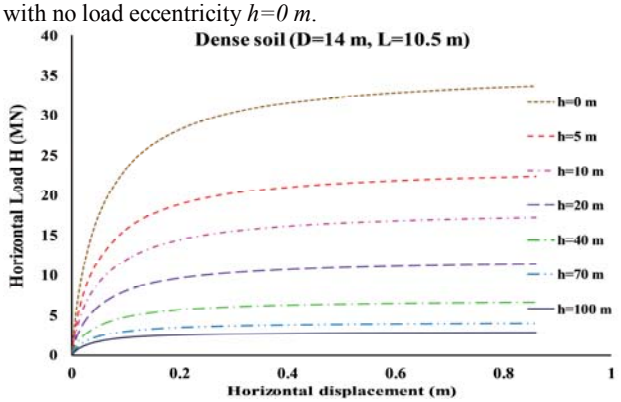

Figure 2. Load-displacement curves for dense sand with embedment ratio *L/D, 0.75*.

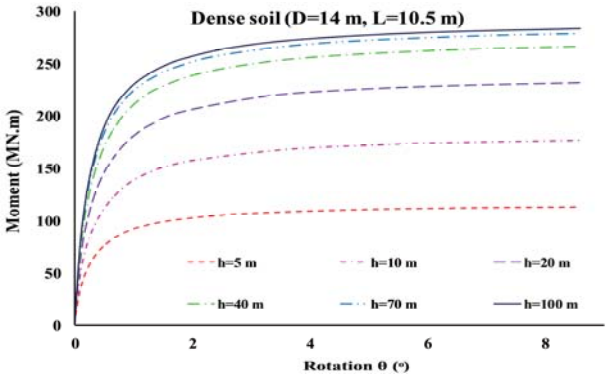

Figure 3. Overturning moment-rotation curves for dense sand with embedment ratio *L/D, 0.75*.

3.2 *Soil response*

Figure 4 shows soil shear stress distribution at both the inside and outside of the bucket for the load eccentricity *h, 100 m*. The stresses concentration is seen at the right inside of the bucket near the tip. It may be explained that by increasing the applied load, due to bucket movement the soil inside of the bucket tends to densify, hence maximum stresses are seen in this area.

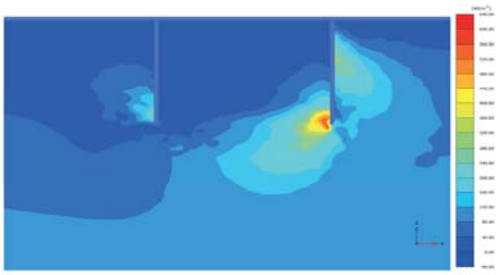

Figure 4. Soil shear stress distribution for dense sand with embedment ratio *L/D, 0.75* and load eccentricity *h, 100 m*.

The soil displacement contour at both the interior and exterior of the bucket for the eccentricity *h, 100 m* is illustrated in Figure 5. It is found that the rotation point appears at a depth of around two-third of the skirt length. Comparison with the results from the load applied at the lower eccentricity represents that increasing the load eccentricity leads to upward movement of the rotation point. Similar behavior can be seen in the pile. The reason for such behavior is that a greater reaction force below the rotation point appears to resist increasing the reaction moment.

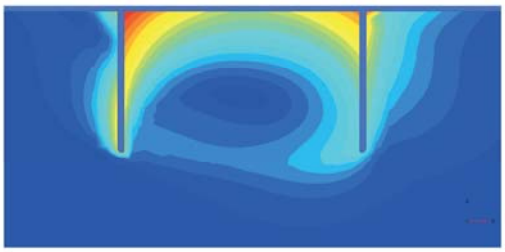

Figure 5. Soil displacement contour for dense sand with embedment ratio *L/D, 0.75* and load eccentricity *h, 100 m*.

Figures 6 and 7 show soil horizontal and vertical displacement for the bucket with the load eccentricity *h, 100 m*. In both figures it is found that maximum soil displacement occurs at the inside of the bucket near the lid. It may be interpreted that with gradually increasing in the horizontal load and overturning moment, the lid only transfers a slight part of load and moment compared to the skirt. Furtheremore, it can be seen a gap below the bucket lid particularly near the left side. Thereby larger soil displacements are seen near the bucket lid areas.

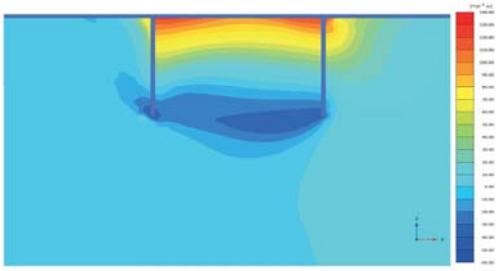

Figure 6. Soil horizontal displacement for dense sand with embedment ratio *L/D, 0.75* and load eccentricity *h, 100 m*.

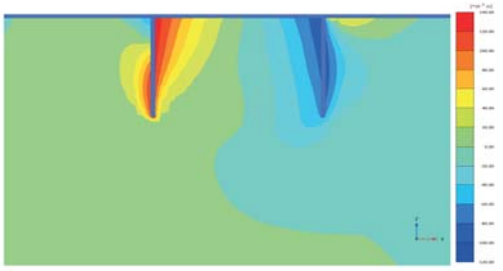

Figure 7. Soil vertical displacement for dense sand with embedment ratio *L/D, 0.75* and load eccentricity *h, 100 m*.

3.3 *Dimensionless curves for load-displacement and moment-rotation relationship*

Regarding dimensionless load-displacement curves, by employing the Power law and using Buckingham's Theorem, the following equation may be obtained:

$$\frac{u}{L}=(\frac{H}{\gamma' L^3})^{\mu}.C \qquad (1)$$

Where μ and C are a constant exponent and coefficient. In order to get a better understanding of the bucket behavior once subjecting to the horizontal load and overturning moment, dimensionless displacement against dimensionless horizontal load curves are plotted on a double logarithmic scale (Figure 8).

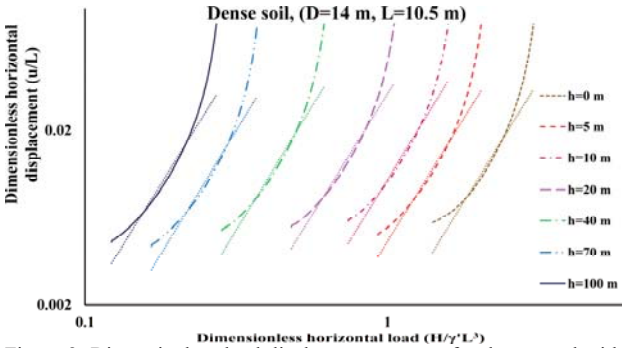

Figure 8. Dimensionless load-displacement curves for dense sand with embedment ratio *L/D, 0.75*.

Two distinct trends can be seen from Figure 8: 1. The first part of each curve can be approximated with straight line distinguished with a certain positive slope; and 2. Utilizing the power law, the aforementioned line can be properly fitted to the FEM analyses data within $0.5H_u$, where H_u is the ultimate horizontal load. After $0.5H_u$, at a certain point the straight lines cease and tend to bend untill failure occurs. Furthermore, considering straight line for the first part, almost a similar slope in all curves are observed. The obtained exponents μ from fitting curves using the Power law were assessed in the range of 2.7-2.8 which can be considered acceptable, due to not existing significant difference.

Likewise, concerning dimensionless form of moment-rotation relationship, similar equation may be obtained applying the Power law and using Buckingham's Theorem:

$$\theta=(\frac{M}{\gamma' L^4})^{\nu}.E \qquad (2)$$

Where ν and E are a constant exponent and coefficient, respectively. Figure 9 displays the dimenwesionless overturning moment-rotation curves on a double logarithmic scale.

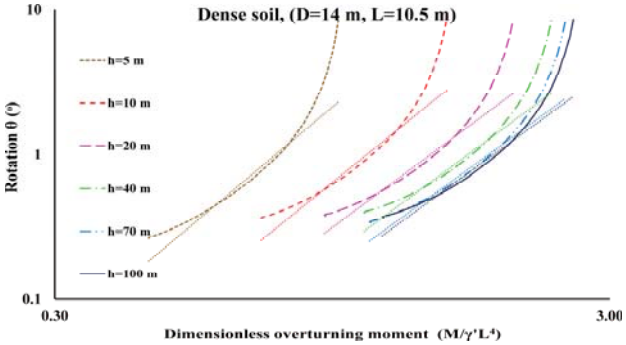

Figure 9. Dimensionless overturning moment-rotation curves for dense sand with embedment ratio *L/D, 0.75*.

From fitting curves and by using the Power law, the obtained exponents ν befall within the range of 2.7-3.1 that can also be considered acceptable.

3.4 *Ultimate horizontal load-overturning moment diagrams*

For the given bucket dimensions, ultimate horizontal load-overturning moment capacity diagrams (H_u-M_u) are presented in Fig. 10.

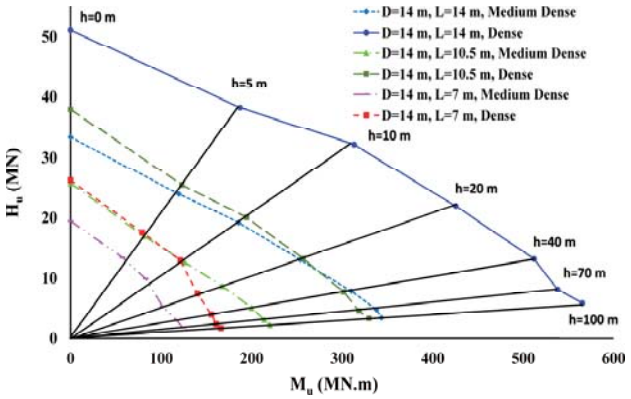

Figure 10. Ultimate horizontal load-overturning moment diagrams.

From the results, it can be perceived that the ultimate horizontal load and overturning moment capacity are substantially influenced by the bucket geometry and soil density. The horizontal load and moment capacity increase with increasing the embedment ratio.

3.5 *Normalized ultimate horizontal load-overturning moment diagrams*

To take into account the effect of bucket geometry on the load and moment capacity, both bucket diameter and skirt length with different weights were considered to determine dimensionless variables. Evidently, no clear trend was not observed by using above-mentoioned dimenssionless variables. Thereby, modified terms were sought that enable finding a general expression for the normilized ultimate load and moment capacity in the suction bucket foundation for the given soil types. The following equations express the normalized ultimate horizontal load and overturning moment considering mentioned modification:

$$\overline{H_u} = \left(\frac{H_u}{\gamma' L^2 D}\right)\left(\frac{L}{L_{ref}}\right)^{0.9} \quad (3)$$

$$\overline{M_u} = \left(\frac{M_u}{\gamma' L^3 D}\right)\left(\frac{L}{L_{ref}}\right)^{0.4} \quad (4)$$

Where L_{ref}=*1 m*. Figure 11 shows modified normalized ultimate horizontal load-overturning moment diagramS.

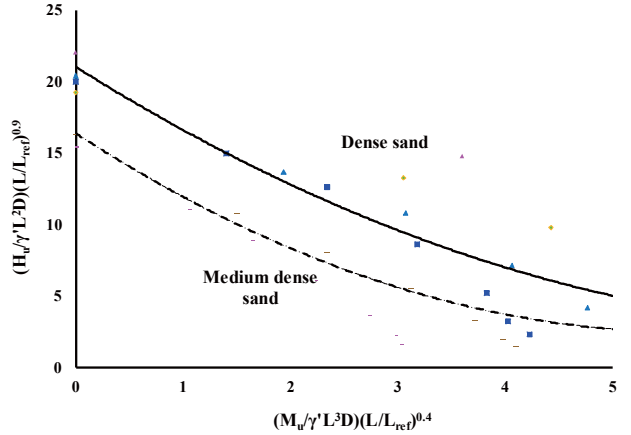

Figure 11. Modified normalized ultimate horizontal load-overturning moment diagramS.

The given figure can be utilized for the preliminary design to find a suitable bucket geometry.

4 CONCLUSION

This paper presents three-dimensional analyses results for suction bucket foundation used for offshore wind turbines. From the present paper the following conclusions can be drawn:
The analysis of numerical simulation results show that only a small part of the applied loads are endured by the bucket lid while bucket skirt bears a major part of the operational loads, hence maximum vertical and horizontal soil displacements are seen near the bucket lid.
Due to bucket movement and soil densification, the maximum values of the soil stresses are seen near the bucket tip at the right inside of the bucket.
The Power law had a good agreement with the obtained numerical analysis results until a certain value of the horizontal load and overturning moment.
Bucket rotation and displacement are drastically dependant on the bucket dimenstions and soil density.
The normalized horizontal load-overturning moment diagaram may be used for the prepratory design of the bucket foundations used for offshore wind turbines.
Some other widely unsolved aspects of the bucket bearing behavior like the effect of the installation procedure and bucket behavior subjected to the cyclic loads, etc. were not considered in current study. Therefore, further research on the bearing behavior of the bucket foundations considering all unsolved aspects are needed.

5 ACKNOWLEDGEMENTS

This research was supported by Basic Science Research Program funded by the National Research Foundation of Korea. We thank the support (NRF-2017R1A2B4010201).

6 REFERENCES

Achmus M. Akdag C.T., Thieken K., Load-bearing behavior of suction bucket foundations in sand. Applied Ocean Research´ 2013; (43):157–165

Bye A, Erbrich CT, Rognlien B, Tjelta TI. 1995. Geotechnical design of bucket foundations. Proceedings of Offshore Technology Conference (OTC); Houston, TX. 16 p.

Byrne, B.W. and Houlsby, G.T. (2004). Experimental investigations of the response of suction caissons to transient combined loading. Journal of Geotechnical and Geoenvironmenal Engineering, ASCE, 130 (3), 240-253.

Villalobos FA, Byrne BW, Houlsby GT. An experimental study of the drained capacity of suction caisson foundations under monotonic loading for offshore applications. Soils and Foundations 2009;49:477–88.

Houlsby GT, Ibsen LB, Byrne BW. Suction caissons for wind turbines. In: Proceedings of international symposium on frontiers in Geotechnics: ISFOG, Perth, Australia. 2005, pp. 75–94.

Houlsby GT, Byrne BW. Suction caisson foundations for offshore wind turbines and anemometer masts. Journal of Wind Engineering, 24 (2000), pp. 249–255.

Zhang JH, Chen ZY, Li F. Three dimensional limit analysis of suction bucket foundations. Ocean Engineering 2010;37:790–9.

Brinkgreve, Engin, and Swolfs, 2012. R.B.J. Brinkgreve, E. Engin, and W.M. Swolfs. Manual for PLAXIS 3D 2012, 2012.

Tae Gyung Ryu, 2015. Long-term Dynamic Behavior Study of Marine Silty Sand for Offshore Structure Foundation Design. Master thesis.